PREDICTION, OPTIMIZATION AND PRODUCTION OF THE PERFORMANCE INDICATORS OF AN IMPROVED LOCALLY PRODUCED HYBRID BRAKE PAD

Oladapo Babafemi, FAKIYESI*
Industrial and Production Engineering
Nnamdi Azikiwe University
Awka
Anambra State
Nigeria
+2348034826047
bo.fakiyesi@unizik.edu.ng

Joseph Ifeanyi, ACHEBO
Production Engineering
University of Benin
Benin City
Edo State
Nigeria
joseph.achebo@uniben.edu

Kessington, OBAHIAGBON
Chemical Engineering
University of Benin
Benin City
Edo State
Nigeria
kess.obahiagbon@uniben.edu

Frank Omos, UWOGHIREN
Production Engineering
University of Benin
Benin City
Edo State
Nigeria
frank.uwoghiren@uniben.edu

ABSTRACT

In order to improve and enhance the production of automotive brake pad for better friction reduction, the materials that are practically made of reinforced composites should possess optimum physical and mechanical properties. These properties which consist of minimum wear rate, higher coefficient of friction, higher porosity and adequate surface hardness expected to produce optimal values. This study focused on the prediction and optimization of performance indicators of a locally made hybrid brake pad. Combinations of coconut shell, boron dust and corn husks were used as filler materials; phenolic resin as a binder; graphite as lubricant; silicon carbide plus copper as abrasives. During experimental studies, surface hardness (SH), specific wear rate (SWR) and porosity (P) was also measured. Optimization tools such as Design Expert, MINITAB, and SPSS were used for optimum material selection and process analysis. Also, responses' reduction efficiency were obtained at P 18.792%*, SH* $78.220hr/s$ *and SWR* $15.510 \times 10^{-6}NM^{-3}/Nm$*. The reduction efficiency was predicted based on desirability function of* 0.781*. The reinforced composites produced a relative density of* $1.17g/cm^3$ *and the mixtures were specifically measured in proportions. Accuracy measurements gave the value of MAPE for the model as* 33.1403*, MAD (*0.053*) and MSD (*0.004*).*

KEYWORDS: *Prediction, Optimization, Hybrid, Brake Pad, Filler Materials, Binders, Friction Modifiers, Reinforcement and Composites.*

1. INTRODUCTION

Brake pads are part of the components that convert the kinetic energy of a vehicle to thermal energy through friction [1]. Two brake pads are contained in the brake with their friction surfaces facing the rotor. During the hydraulic application of the brake, the caliper clamps or squeezes the two pads together onto the spinning rotor to slow and stop the vehicle. When a brake pad heats up due to contact with the rotor, it transfers small amounts of its friction material onto the disc, leaving a dull grey coating on it. The brake pad and disc (now both having the friction material), then "stick" to each other, providing the friction that stops the vehicle [14]. The braking system is one of the most important parts of any vehicle (i.e., car, bus, train, airplane, etc.) because the braking system's failure can lead to very serious accident which might even claim lives. Brake pads are designed mainly to achieve friction stability, durability, minimization of noise and vibration. Thus, the typology of the brake pads depends on the material which they are made [5]. From the past survey, there has been a stringent consumer's awareness towards new products from renewable sources for improved automotive brake pad production [11]. New directives on recycling, social influence and change of cognitive values have led the consumer towards environmentally friendly products. In particular, composite materials are being developed and redesigned in different variations aiming to improve and adapt traditional products by introducing new products to achieve sustainable and responsible brake pads [8].

Furthermore, state-of-the-art brake pads are constituted nowadays by resin-bonded composite friction materials, these are specially formulated to give good friction and wear performance [2]. Research in recent times has been geared towards the use of industrial and agricultural waste as raw materials for the production of various engineering materials of which the production of brake pads has had a fair share. The carcinogenic and other health related effects associated with use of asbestos in brake pads production has called for the need for replacement of materials that provide brake pads with good mechanical properties [13]. A number of material-processing strategies have been used to improve the wear performance of polymers composite. Glass fiber reinforced polymeric composites traditionally show poor wear resistance and high friction due to the brittle nature of the reinforcing fibers. This has prompted many researchers to cast the polymers with fibers/fillers [10].

Boron is metalloid which is very commonly used in the industry. It is characterized by a high melting point. Also, it demonstrates low chemical activity. Boron is a good thermal and electrical isolator. Due to its advantageous properties, it was categorized as a friction material [12]. Boron fraction in brake pads usually does not exceed 2% of volume. It is hard and therefore improves the durability of the pad, which corresponds to increased wear resistance [4]. Thus, this research was to predict and optimize the performance indicators of the locally made hybrid brake pad using optimization tools like; Minitab 16, SPSS and Design Expert.

2. METHODS

An average brake pad comprises of 10 to 20 different substances [6]. Selecting the right composition for the brake pad and predicting its impact on the final products require critical and robust approach. It requires tremendous amounts of research and abundant experience. The decision must also take into account the intended use of the brake pad, and their operating conditions. The formulations of the base materials (i.e. Boron Dust, Coconut Shell and Corn Husks) were subjected to treatments. It has already been observed that molding pressure, molding temperature, molding time, heat treatment time and heat treatment temperature that formed the input parameters play critical roles during the manufacturing of friction materials. Appropriate settings of those process parameters not only help in achieving the desired characteristics of the end products but also save manufacturing time and cost with gave birth to porosity, surface hardness and specific wear rate at output parameters as reported in this study.

There was a theory propounded by [7] that selection of ideal material combination and development was not a simple task but a gradual process involving different material selection stages. Furthermore, two methods for material selection were introduced. These are the Cost per Unit Property of a material and Digital Logic Methods. These two methods are represented in Figure 1.

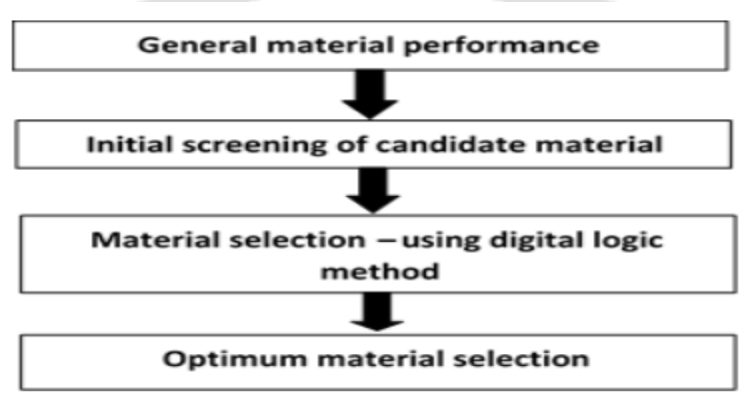

Fig. 1: Material Selection Flow Chart [9]

The application potentialities of some MCDM techniques, i.e., Entropy Method, TOPSIS and EDAS according to [3] was carefully explored while solving two different parametric optimization problems for friction materials in automotive brake applications. To optimally address the aforementioned parameters (input and output) this study made use of Design Expert approach. This offers comparative tests, screening, characterization, optimization, robust parameter design, mixture designs and combined designs.

3. RESULTS

Process analysis and optimization was carried out effectively and presented accordingly. The process analysis identifies the weaknesses and provides opportunity for improvement while the process optimization improves the efficiency and production processes.

Each of the three (3) response parameters in this work was therefore analyzed and modeled accordingly.

3.1 Analysis of Porosity (P)

TABLE I: Fit Summary for (P)

Source	Sequential p-value	Lack of Fit p-value	Adjusted R^2	Predicted R^2	
Linear	0.5562	0.7566	-0.0182	-0.1762	
2FI	0.0762	0.8882	0.2079	-0.3711	
Quadratic	**0.0536**	**0.9676**	**0.3728**	**-0.2647**	**Suggested**
Cubic	0.9676		-0.3685		Aliased

Table I gave the fit summary values of porosity with Quadratic model suggested as the most suitable with the least sequential p-value.

TABLE II: Fit Statistics for (P)

Std. Dev.	**3.02**	**R^2**	**0.7327**
Mean	13.95	**Adjusted R^2**	0.1728
C.V. %	21.63	**Predicted R^2**	0.0641
		Adeq Precision	6.3714

The **Predicted R^2** of 0.0641 is in reasonable agreement with the **Adjusted R^2** of 0.1728; i.e. the difference is less than 0.2. **Adeq Precision** measures the signal to noise ratio. A ratio greater than 4 is desirable. The ratio of 6.3714 indicates an adequate signal. This model can be used to navigate the design space.

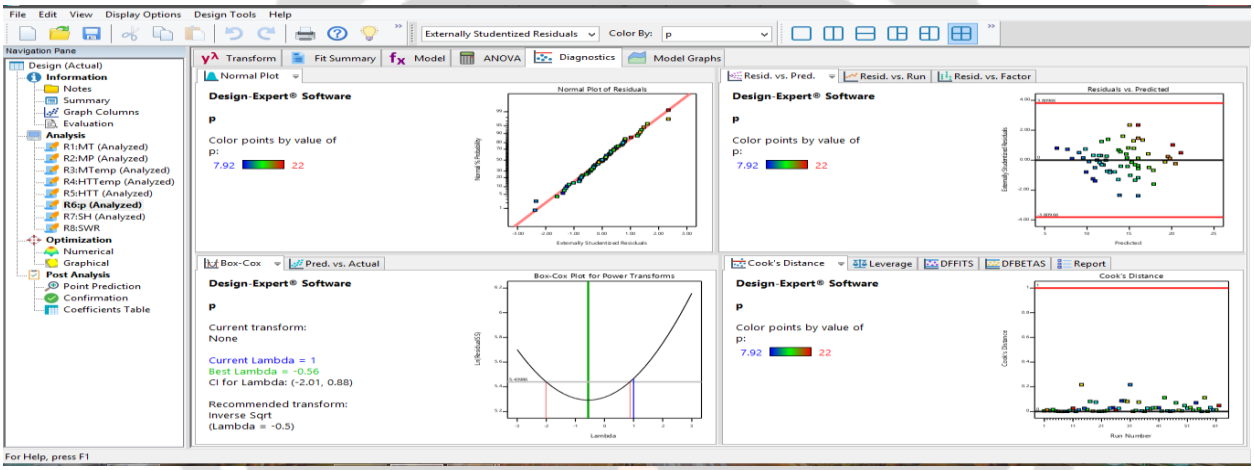

Fig. 2: Normal Plots for (P)

Fig 2 shows the observed value on one axis (usually the horizontal axis) and the value that is expected since the data are a sample from the normal distribution on the other axis. The points clustered around a straight line for a normally distributed variable. If the data are skewed, the normal probability plot will have a very distinctive shape.

TABLE III: Model Comparison Statistics for (P)

PRESS	**1119.22**
-2 Log Likelihood	258.97
BIC	407.55
AICc	437.53

Table III shows the comparison statistics for porosity. In this regard, the significant advantage of the flexibility of the model comparison approach allows the reduction in the number of parameters of a model greatly.

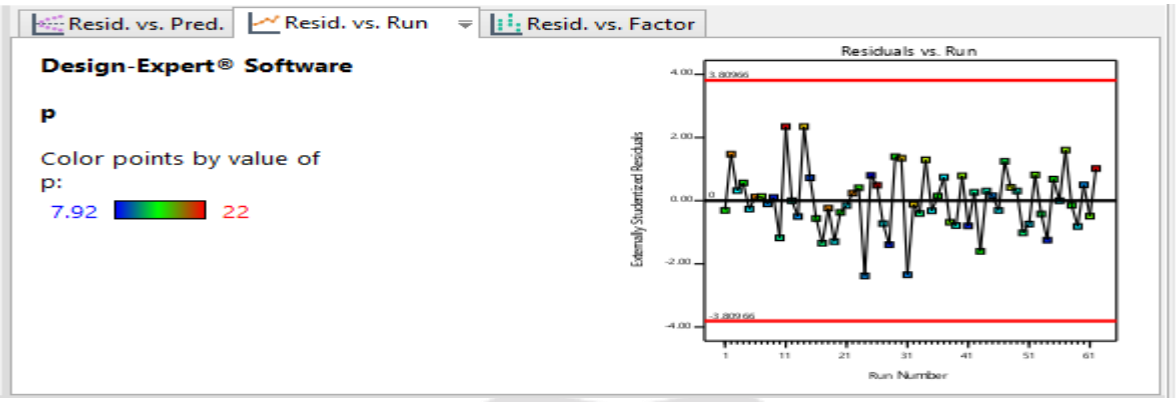

Fig. 3: Residuals Plot for P

The plot in Fig 3 shows that the fitted values of response are in high correlation with the *actual* values, which demonstrates an adequate signal for regression model.

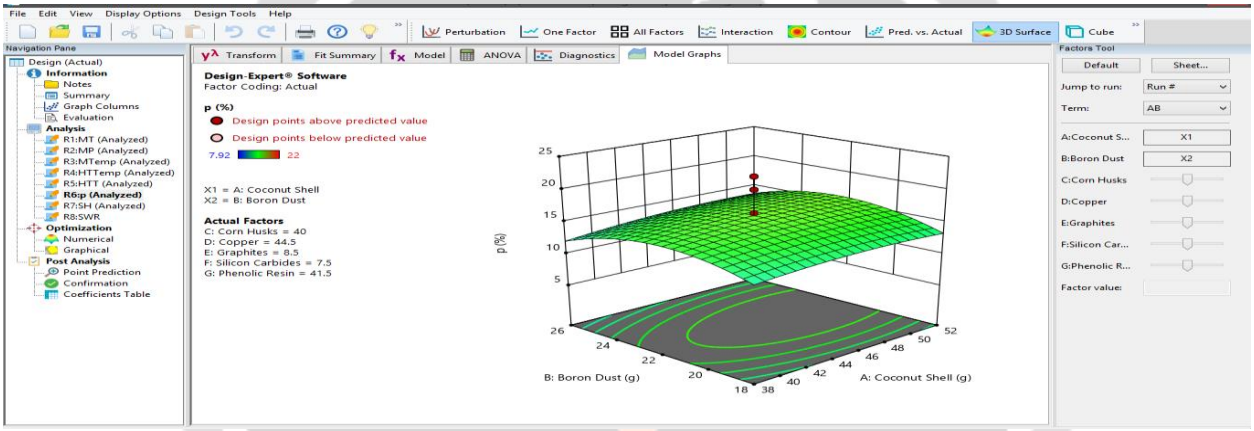

Fig. 4: 3D Surface Plot for P

A surface plot is constructed from three variables as demonstrated in Figure 4. The X and Z (independent) variables are shown on the horizontal axes. The Y variable is shown along the vertical axis. Note that all three variables must be numeric.

3.2 Analysis of Surface Hardness (SH)

TABLE IV: Fit Summary for (SH)

Source	Sequential p-value	Lack of Fit p-value	Adjusted R^2	Predicted R^2	
Linear	0.4283	0.4531	0.0022	-0.1694	
2FI	0.1195	0.5707	0.1836	-0.6051	
Quadratic	**0.0094**	**0.8360**	**0.4639**	**-0.2416**	**Suggested**
Cubic	0.8360		0.1755		Aliased

Quadratic model was also suggested for surface hardness that has the least sequential p-value as shown in Table IV. Adjusted R-squared and predicted R-squared have a reasonable level of agreement (within 0.2 of each other).

TABLE V: Fit Statistics for SH

Std. Dev.	**15.43**	**R^2**	**0.7715**
Mean	87.67	**Adjusted R^2**	0.4639
C.V. %	17.60	**Predicted R^2**	0.3416
		Adeq Precision	7.9509

From Table V, the **Predicted R^2** of 0.4639 is in reasonable agreement with the **Adjusted R^2** of 0.3416; i.e. the difference is less than 0.2. **Adeq Precision** measures the signal to noise ratio. A ratio greater than 4 is desirable. The ratio of 6.3714 indicates an adequate signal.

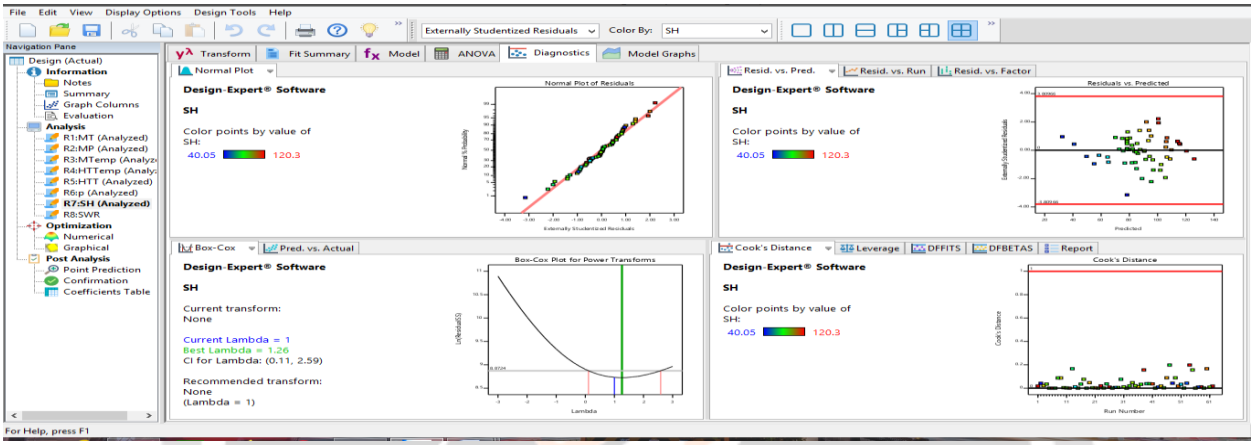

Fig. 5: Normal Plots for SH

Observing from Fig. 5, it can be seen that the points are reasonably close to the line and there are no indications of systematic deviations from the line, thereby indicating that the distribution of the population is reasonably close to normal.

TABLE VI: Model Comparison Statistics for (SH)

PRESS	**33654.71**
-2 Log Likelihood	461.41
BIC	609.98
AICc	639.97

Table VI shows the model comparison statistics for surface hardness. The flexibility of the model-comparison approach allows them to test for specific effects on the location parameters while implementing the assumption that slopes are not affected by constraining the estimated slopes to be equal in all conditions.

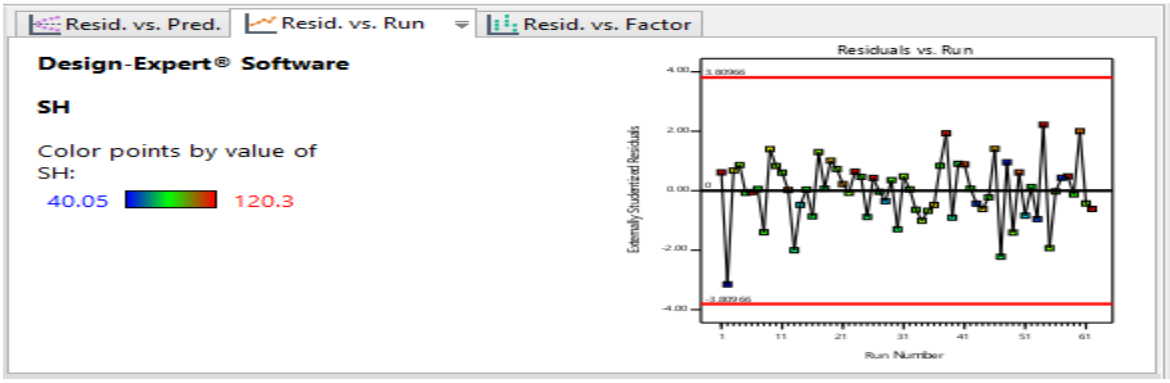

Fig. 6: Residual Plots for SH

Adequacy of the model is further shown from the residual plots as shown in Fig 6, which is the normal probability plot for surface hardness. It can be observed that the residuals follow the normal distribution and the assumption of normality is valid.

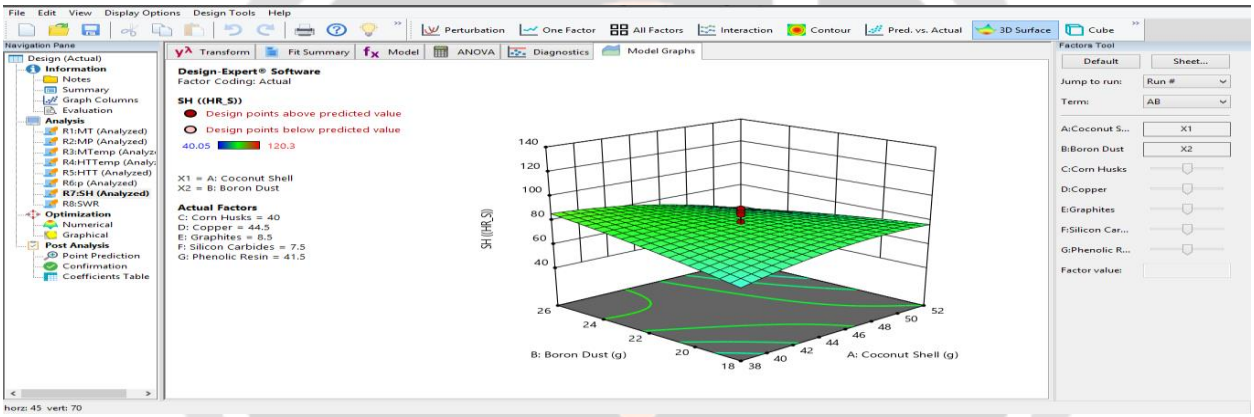

Fig. 7: 3D Surface Plot for SH

This Y value in Fig 7 is a weighted average of all data values that are "near" the grid point. (The number of points averaged is specified to be 120.3). The three-dimensional surface is constructed using these averaged values. Hence, the surface plot does not show the variation at each grid point.

3.3 Analysis of Specific Wear Rate (SWR)

TABLE VII: Fit Summary for Specific Wear Rate (SWR)

Source	Sequential p-value	Lack of Fit p-value	Adjusted R^2	Predicted R^2	
Linear	0.0901	0.5341	0.0922	-0.0668	
2FI	0.1123	0.6622	0.2625	-0.4770	
Quadratic	**0.0216**	**0.7667**	**0.3742**	**-0.4994**	**Suggested**
Cubic	0.7667		0.1450		Aliased

Table VII shown the fit summary statistics for specific wear rate, all model terms' effects are calculated by the program. It produced statistics such as p-values, lack of fit and R-squared values for comparing the models where Quadratic model was suggested with the least sequential p-value.

TABLE VIII: Fit Statistics for SWR

Std. Dev.	**4.06**	**R^2**	**0.7333**
Mean	15.27	**Adjusted R^2**	0.1142
C.V. %	26.59	**Predicted R^2**	0.0994
		Adeq Precision	6.7001

Considering the fit statistics for specific wear rate in Table VII, the **Predicted R^2** of 0.0994 is in reasonable agreement with the **Adjusted R^2** of 0.1142; i.e. the difference is less than 0.2. **Adeq Precision** measures the signal to noise ratio. A ratio greater than 4 is desirable. The ratio of 6.7001 indicates an adequate signal. This model can be used to navigate the design space.

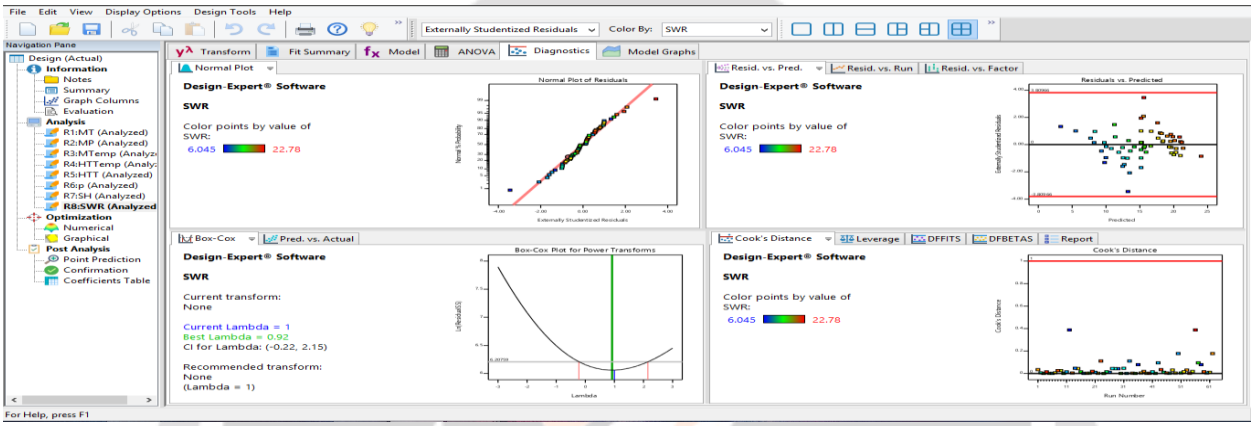

Fig. 8: Normal Plots for SWR

It can be observed in Fig 8 that the residuals follow the normal distribution and the assumption of normality is valid.

TABLE IX: Model Comparison Statistics for SWR

PRESS	**2409.13**
-2 Log Likelihood	295.82
BIC	444.39
AICc	474.38

Table IX is the model comparison statistics for specific wear rate. By the principle of parsimony one should select the most restrictive assumptions that can reasonably expect to be valid. Another factor to consider is whether the data contain sufficient information to estimate the slope parameter which was ascertained.

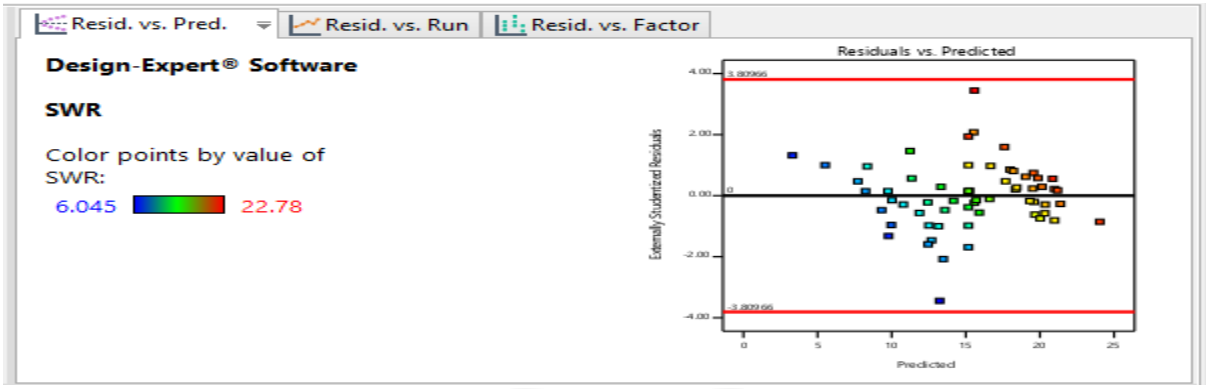

Fig. 9: Residual Plot for SWR

Figure 9 is a plot of the residuals versus the predicted response values. The constant variance shows that the plot is randomly scattered and the residuals has a constant range.

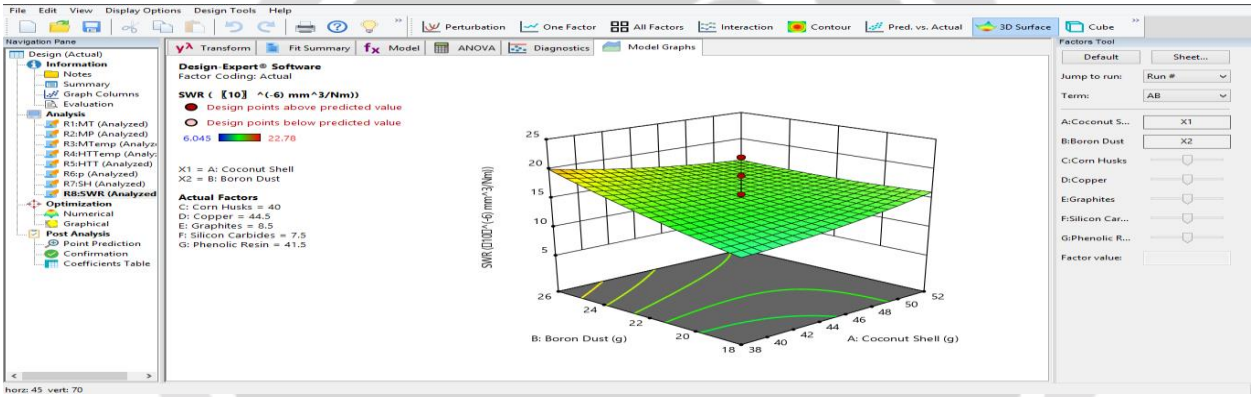

Fig. 10: 3D Surface Plot for SWR

The plot in Fig 10 is useful in regression analysis for viewing the relationship among a dependent and two independent variables. The multiple regressions assumed that this surface is a perfectly flat surface. Hence, the surface plot visually indicates that the multiple regressions are appropriate.

3.4 Process Optimization

Optimization analysis is one the methods employed in this study which is a method of optimizing the subject under a variety of predefined physical constraints. There are several types of optimization methods and their use requires an understanding of the subject, system of constraints and a general direction for the solution. Optimization tools enabled the improvement of design stages, shortening convergence processes and streamlining development stages.

3.4.1 Numerical Responses

Numerical optimization is another technique used to determine the optimum conditions of the operating variables in this study. In addition to the design points, a set of random points are checked to see if there are more desirable solutions.

TABLE X: Design Constraints

Name	Goal	Lower Limit	Upper Limit	Lower Weight	Upper Weight	Importance
A:Coconut Shell	maximize	38	52	1	1	3
B:Boron Dust	maximize	18	26	1	1	3
C:Corn Husks	maximize	36	44	1	1	3
D:Copper	maximize	41	48	1	1	3
E:Graphites	maximize	5	12	1	1	3
F:Silicon Carbides	maximize	4	11	1	1	3
G:Phenolic Resin	maximize	35	48	1	1	3
P	maximize	7.92	22	1	1	5
SH	maximize	40.05	120.3	1	1	5
SWR	maximize	6.045	22.78	1	1	1

Maximization goal was employed where the lower limits are the lowest acceptable outcomes and the upper limits are desired best results. Based on the response surface and desirability function, optimal values for the factors' reduction efficiency were obtained and recorded.

3.4.2 Graphical Responses

Graphical optimization displays the area of feasible response values in the factor space.

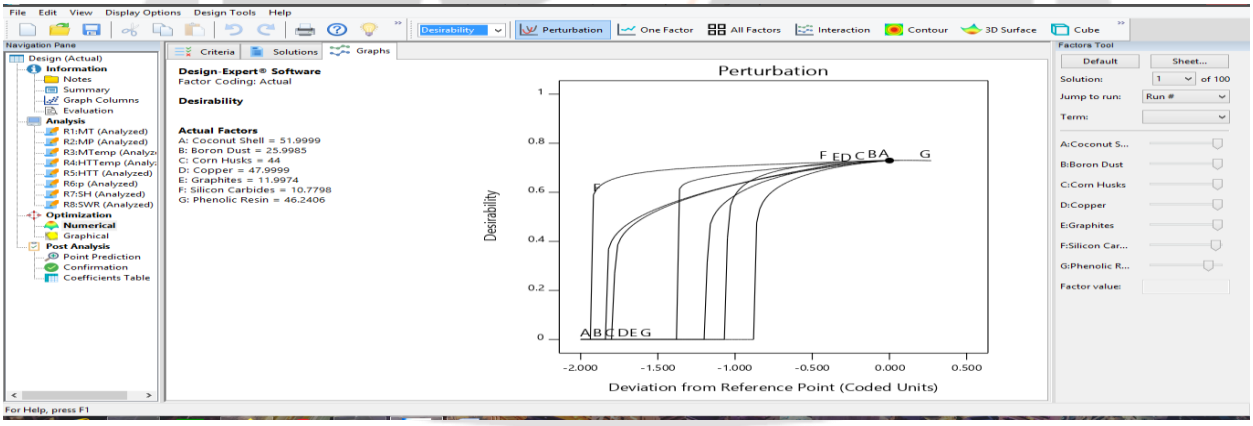

Fig. 11: Desirability Curve for the Factors

Based on the desirability method, the analysis has been performed. The attained perturbation graph of desirability (Fig. 11) displays that the arrangement of process parameter levels consuming the maximum desirability of 0.781 of the actual factors is optimal.

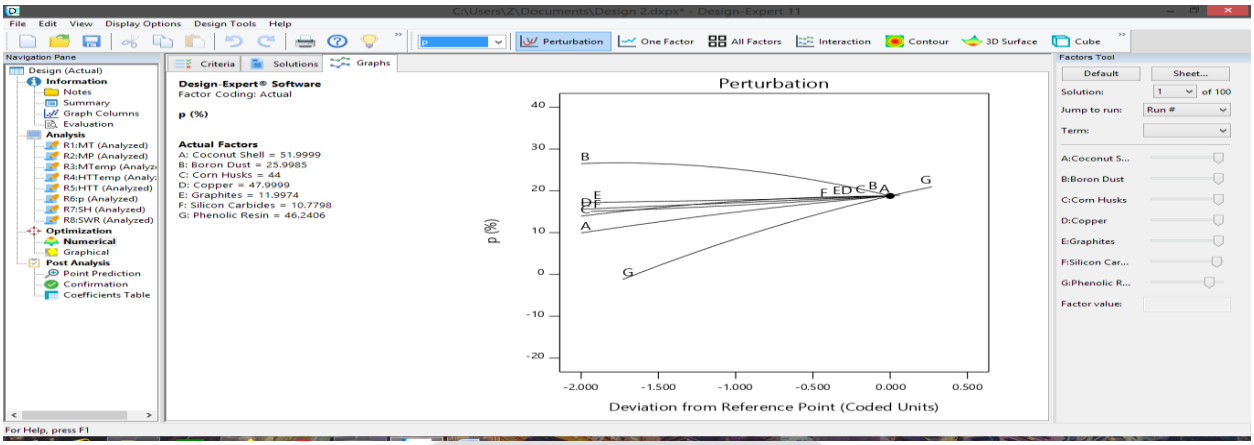

Fig. 12: Desirability Curve for P

Selected points with the highest desirability values for porosity (P) response are shown in Fig 12.

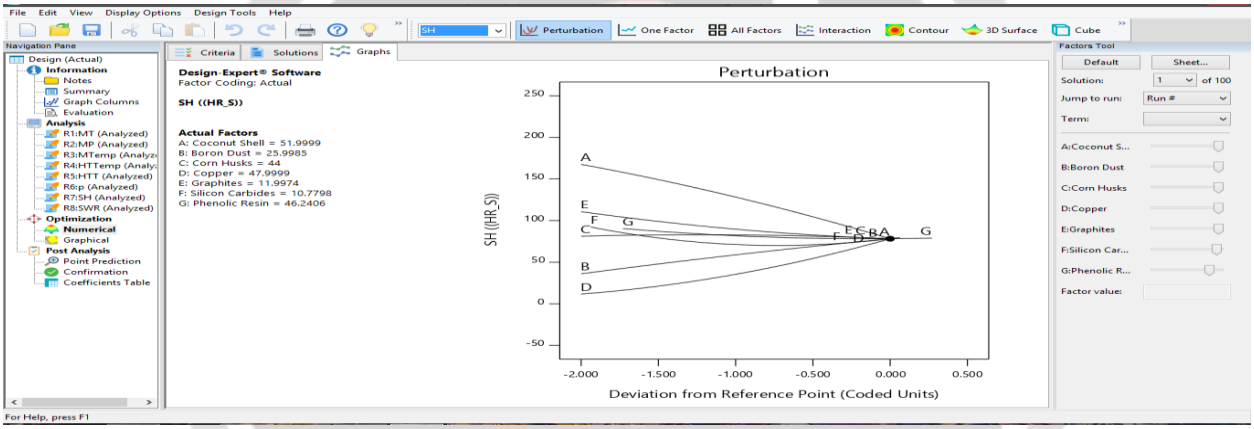

Fig. 13: Desirability Curve for SH

Figure 12 show the overall desirability for this solution that gave a value of 18.792. All responses are predicted to be within the desired limits. This confirmed the optimal solution, indicating that small variations around $\boldsymbol{x}^*$ are predicted to not change the overall desirability drastically.

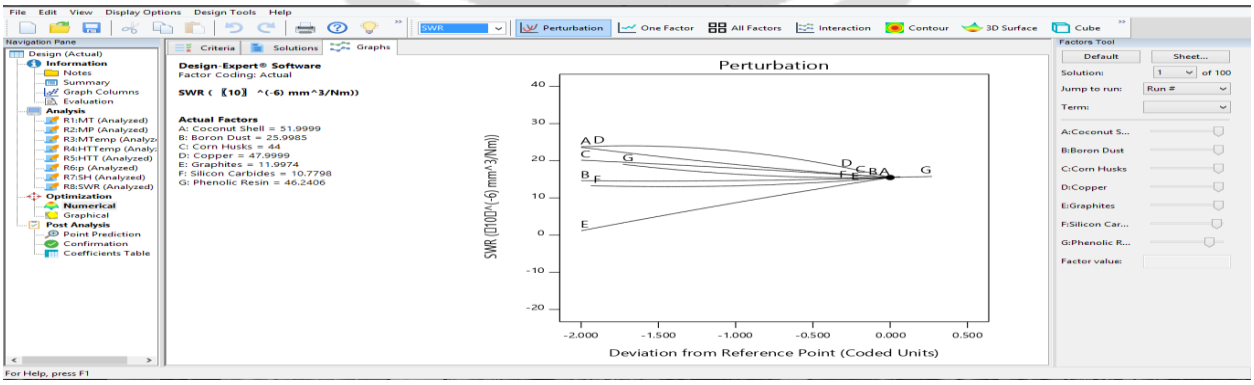

Fig. 14: Desirability Curve for SWR

Figure 14 maximized desirability such that the experimental factors are constrained to be within a spherical design region with a radius equal to the axial point distance. The High control point is positioned at the maximum Y value and aligned at the high desirability, close to 1. The Low control point is positioned at the minimum Y value and aligned at a low desirability, close to 0.

TABLE XI: Point Prediction

Solution 1 of 100 Response	Predicted Mean	Predicted Median	Observed	Std Dev	SE Mean	95% CI low for Mean	95% CI high for Mean	95% TI low for 99% Pop	95% TI high for 99% Pop
P	18.7916	18.7916		3.01632	5.01387	8.4855	29.0978	-1.06292	38.6462
SH	78.2202	78.2202		15.4344	25.6558	25.484	130.956	-23.375	179.815
SWR	15.5103	15.5103		4.06003	6.74877	1.63805	29.3826	-11.2143	42.235

A prediction interval summary was displayed in Table XI which shows larger values than the confidence interval because there are more scattered points expected from a small sample that estimates the average versus the entire population's true mean.

TABLE XII: Model Confirmation

Solution 1 of 100 Response	Predicted Mean	Predicted Median	Observed	Std Dev	N	SE Pred	95% PI low	Data Mean	95% PI high
P	18.7916	18.7916		3.01632	1	5.85124	6.76425		30.8191
SH	78.2202	78.2202		15.4344	1	29.9406	16.6764		139.764
SWR	15.5103	15.5103		4.06003	1	7.8759	-0.678796		31.6995

Model Confirmation in Table XII was intended to be used to confirm that the model can predict actual outcomes at the optimal settings determined from the analysis. Additional (n) runs are conducted at the optimal settings. The average of those runs is compared to the prediction interval for a sample of size n.

4. DISCUSSION

The samples prepared for this study were formulated using the rule of mixture. The practical density that was gotten from the samples through the rule of mixture theorem indicates that the combination of Coconut Shell, Boron Dust and Corn Husks as reinforced composites produced a relative density of $1.17 g/cm^3$.

Figures 2, 5 and 8 represented the normal plots for the responses. In the normal distributions, the data was symmetrically distributed with no skew. That is, data was aligned closely to the dotted lines which indicate a normal distribution. These are the scatterplots with the quartiles of the scores on the horizontal axis and the expected normal scores on the vertical axis.

The graphical plots and statistical test of the residuals are examined and presented in Figures 3, 6 and 9. Judgments are made based on these examinations which further confirmed the validity of the models. The residuals are estimates of experimental error obtained by subtracting the observed responses from the predicted responses.

The percentage contribution of each control factor is employed to measure the corresponding effect on the quality characteristic. Tables I, II, IV, V, VII and VIII showed the results of the statistics with the model responses. These

analyzes was undertaken for a level of significance of 5% that is, for level of confidence 95%. The parameters in the fits summary tables indicate the order of significance among factors and interactions. These statistical values are presented as; P ($p - value = 0.0536$), SH ($p - value = 0.0094$) and SWR ($p - value = 0.0216$).

From Response Surface Regression Parameters as shown in design constraints Table X, this model responses exhibit first-order regression model across all the statistical parameters which is the reason for the fitted response surface to be plane. The optimal values for the factors' reduction efficiency were obtained and recorded.

From the desirability curves in Figures 11, 12, 13 and 14, the overall desirability for this solution is 0.781. All responses are predicted to be within the desired limits. The model shows optimal solution, indicating that small variations around $\boldsymbol{x}^*$ are predicted to not change the overall desirability drastically. Thus, minimum specific wear rate for the developed composites is obtained when the sliding velocity and normal load are at the lowest level, also filler content and sliding distance are at the highest level.

5. CONCLUSION

The locally made hybrid brake pads of an automotive brake system are designed by first, determining its frictional materials, ascertain the wear behavior of the materials selected and finally modeled the output responses to determine how it affects the performance. These performance indicators has been analyzed and optimized to compete favorably with mechanical properties of commercial brake pads.

6. REFERENCES

[1]. T. Aitana, R. Fausto, P.A. Roberto, S. R. Leticia and R. Juan., 2021, "Preparation and Properties of Sustainable Brake Pads with Recycled End-of-Life Tire Rubber Particles".

[2]. K. Naveen, B. Ajaya, H.S. Goyal and K.P. Kunvar., 2021, "The Evolution of Brake Friction Materials; A Review" Materials Physics and Mechanics. 47(5): 796-815. DOI: 10.18149/MPM. 4752021_13.

[3]. C.U. Nwogu and J.O. Osarenmwinda., 2021, "Response Surface Modeling of an Automobile Brake Pad Made from a New-Fangled Composite Material" NIPES Journal of Science and Technology Research 3(3) pp.89 - 103 pISSN-2682-5821, eISSN-2682-5821.

[4]. OAK RIDGE NATIONAL LABORATORY., 2021, "Compositions, Functions, and Testing of Friction Brake Materials and Their Additives" Oak Ridge, Tennessee 3783 l-6285.

[5]. K. Vignesh, K. Anbazhagan, E. Ashokkumar, R. Manikandan, and A. Jayanth., 2015, "Experimental Analysis of Mechanical Properties of Sea Shell Particles– Polymer Matrix Composite" International Journal of Mechanical and Industrial Technology, 3(1)13–21.

[6]. Wikipediacontributors.Brakepad.In *Wikipedia, TheFreeEncyclopedia*.Retrieved16:40,October29,2023 https://en.wikipedia.org/w/index.php?title=Brake_pad&oldid=1181482751

[7]. A. Ashalwan and B.F. Yousif., 2013, "In State of Art: Mechanical and Tribological Behaviour of Polymeric Composites Based on Natural Fibers" Materials & Design, 48,14-24.

[8]. O.A. Danladi, S.S. Ibrahim and A.B. Mohammed.., 2020, "A Review on Brake Pad Materials and Methods of Production" Composite Materials. Vol. 4, No. 1, pp. 8-14. doi: 10.11648/j.cm.

[9]. C. Douglas., 2010, "Montgomery, Design and Analysis of Experiments" John Wiley and Sons, New York, NY, USA, 5th edition.

[10]. H. Efendy, W.M. Wan-Mochamad and N.B.M. Yusuf., 2010, "Development of Natural Fiber in Non-Metallic Brake Friction Material" Seminar Nasional Tahunan Teknik Mesin (SNTTM), 13–15, Ke-9 Palembang.

[11]. A. Kholil, S.T. Dwiyati, R. Wirawan and M. Elvin., 2021, "Brake Pad Characteristics of Natural Fiber Composites from Coconut Fiber and Wood Powder" Journal of Physics: Conference Series 2019 (2021) 012068 IOP Publishing. doi:10.1088/1742-6596/2019/1/012068.

[12]. M. Kumar, B.K. Satapathy, A. Patnaik, D.K. Kolluri and B.S. Tomar., 2011, "Hybrid Composite Friction Materials Reinforced With Combination of Potassium Titanate Whiskers and Aramid Fibre: Assessment of Fade and Recovery Performance," Tribology International, vol. 44, no. 4, pp. 359–367.

[13]. K. Lee and K. Park., 2019, "Optimal Robust Control of a Contactless Brake System Using an Eddy Current" Mechatronics. (6): 615-631.

[14]. R.L. Mitra., 2014, "Minimization of Stopping Time of Disc Brake for Passenger Vehicle" Elservier Science.